Electronic Supplementary Material (ESI) for Analyst.

Supporting Information

Probing Propeller-Like Loops of DNA G-quadruplexes with Looped-Out 2-Aminopurine for Label-Free Switchable Molecular Sensing

Pai Peng, Yi Du, Yudie Sun, Shuangna Liu, Lan Mi and Tao Li*

Department of Chemistry, University of Science and Technology of China, 96 Jinzhai Road, Hefei, Anhui 230026 (China); E-mail: tlitao@ustc.edu.cn

Table of Contents

I. Supplementary figures and discussion

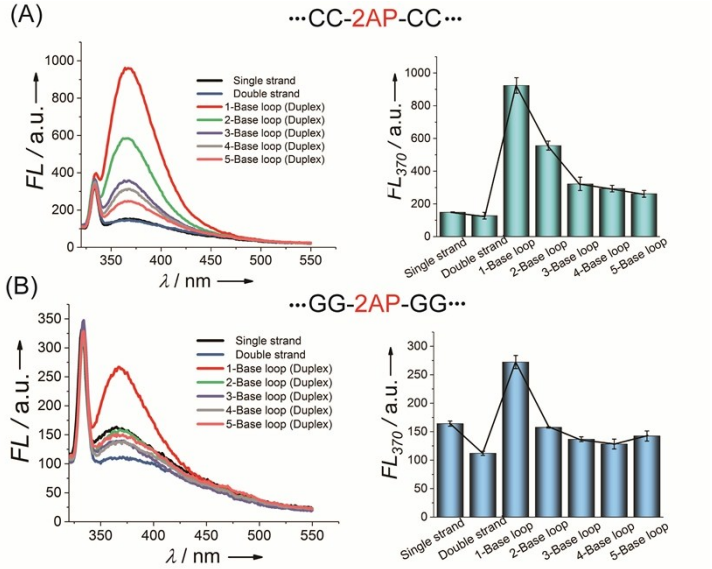

Figure S1. Influence of adjacent loop residues including (A) cytosines and (B) guanines on the fluorescence of looped-out 2-AP in DNA duplexes.

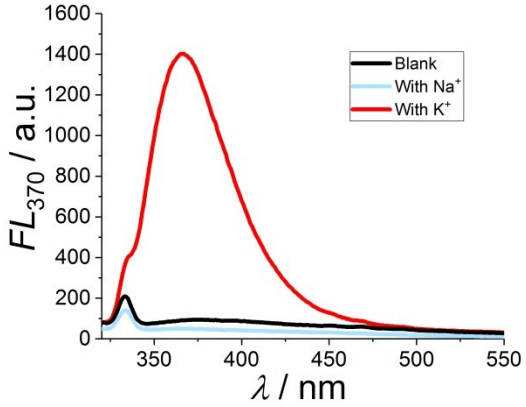

Figure S2. Fluorescence spectra of 2-AP in parallel and antiparallel folded FG9A stabilized by K^+ and Na^+ respectively.

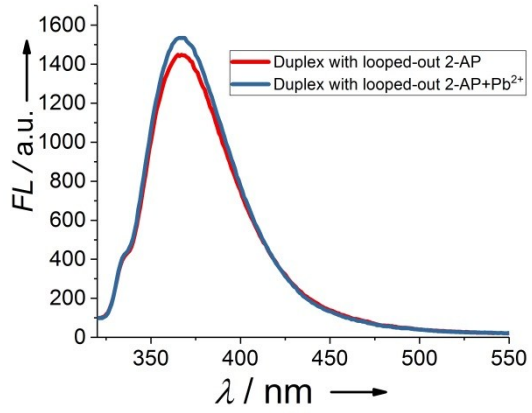

Figure S3. Effect of Pb^{2+} on the fluorescence of looped-out 2-AP in duplex

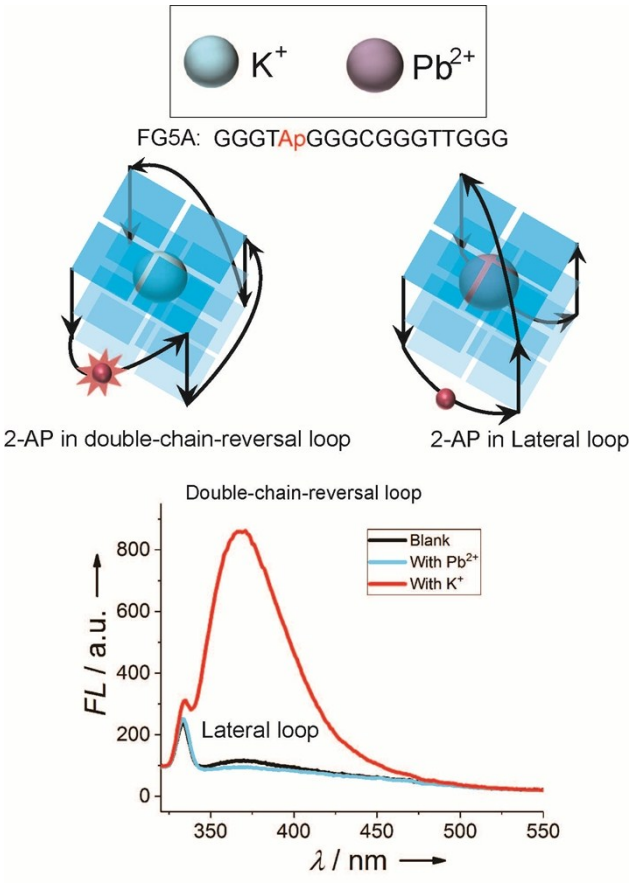

Figure S4. Fluorescence spectra of 2-AP in propeller-like loop and lateral loop by folding FG5A with different ions.

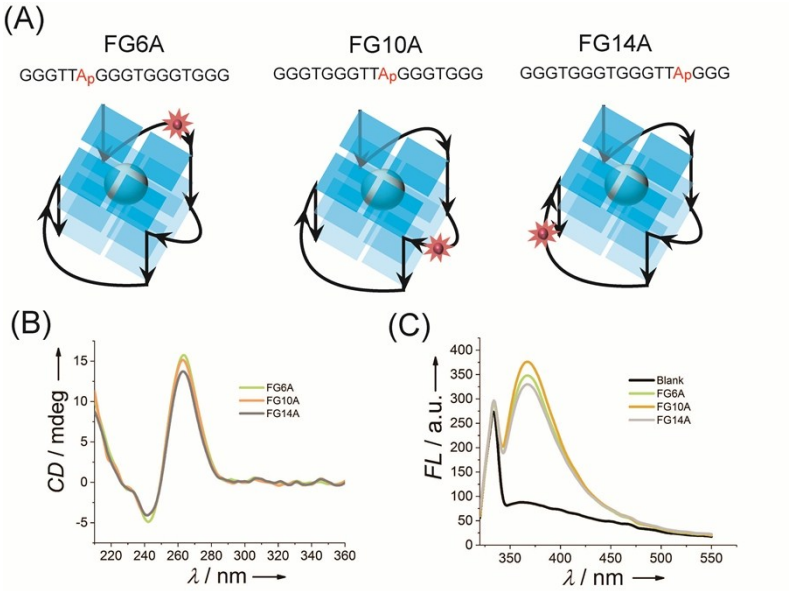

Figure S5. Fluorescence analysis of 2-AP in different loops of parallel G-quadruplexes. (A) Illustration of 2-AP in the first loop (FG6A), the second loop (FG10A) and the third loop (FG14A) in parallel G-quadruplexes. (B) fluorescence spectra (C) CD spectra of 2-AP in each loop.

We further tested whether the fluorogenic 2-AP containing loop is applicable to determine any one of the three propeller-like loops in parallel G-quadruplex. We designed three sequences (FG6A, FG10A, FG14A) adapted from PW17[1], of which each sequence contains a three-base loop when the parallel G-quadruplex is formed in the presence of K^+ (Figure S5A). Similaily, the positive band around 265 nm and the negative one near 245 nm in CD spectra (Figure S5B) in the presence of K^+ show that all the three G-quadruplexes adopt parallel conformation, proving the existence of propeller-like loops in these G-quadruplexes. We next explored the fluorescence performance of 2-AP from the first propeller-like loop to the third one. Indeed, the fluorescence intensity of 2-AP in each loop is around 300 a.u., much the same as that of the 3-base propeller-like loop (Figure S5C vs. Figure 5B), demonstrating that the fluorogenic 2-AP-containing loop is applicable to any one of the three propeller-like loops in parallel G-quadruplex, providing the possibilities to identify G-quadruplex folding topology in human telomeric (3+1) G-quadruplex.

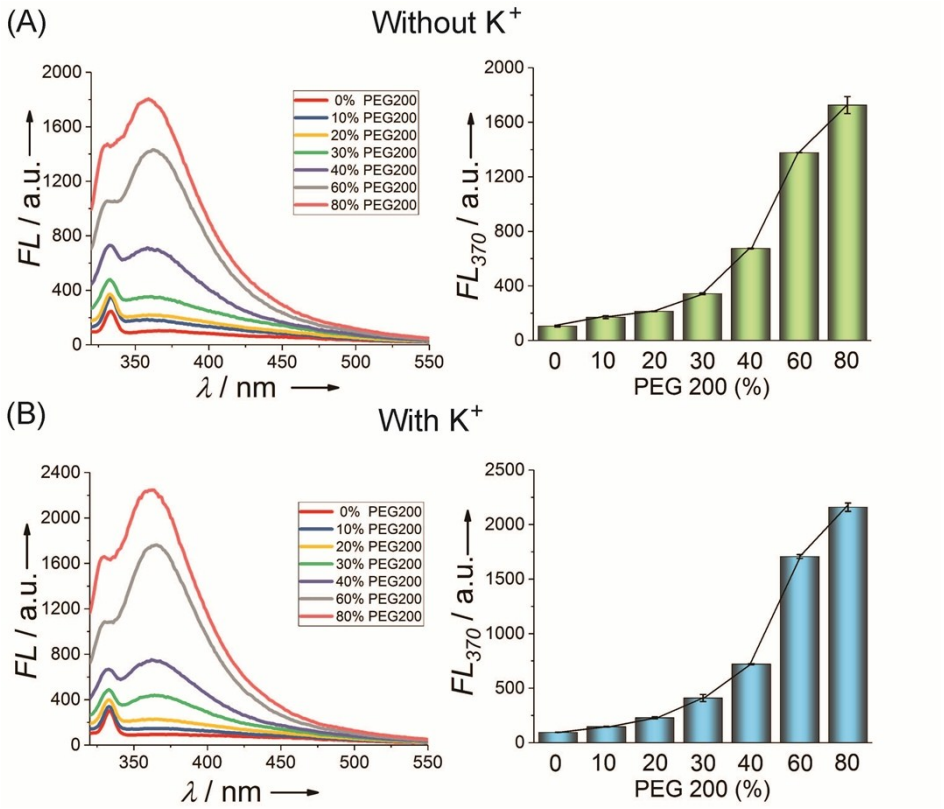

Figure S6. Solvent effect of PEG 200 on the fluorescence properties of the 2-AP incorporated G-quadruplex forming strand (A) In the absence and (B) presence of K^+.

Our presented method is in principle applicable to fast identifying the parallel conformation of human telomeric G-quadruplex by illustrating that all loops are the double-chain reversal. The parallel-stranded human telomeric G-quadruplex has been reported able to be induced from the hybrid type by 40% PEG-200 under molecular crowding conditions in the presence of K^+, reflected by a sharp increase in the 2-AP fluorescence.[2] However, we find that the fluorescence of 2-AP gradually increases with increasing concentrations (0–80%) of PEG-200, independent of cations (Figure S6). Given that 2-AP is greatly influenced by the polarity of the solvent,[3-6] our observations strongly suggest that the fluorescence change upon addition of PEG-200 mainly originates from the solvent effect rather than the structure conversion of

the G-quadruplex. Although the CD spectra were also measured in the absence and presence of PEG-200,[2] it cannot be used alone as a definitive tool for G-quadruplex structural classification,[7] as CD only reports on base stacking environment rather than strand polarity and thus causes false positive results.[7-10]

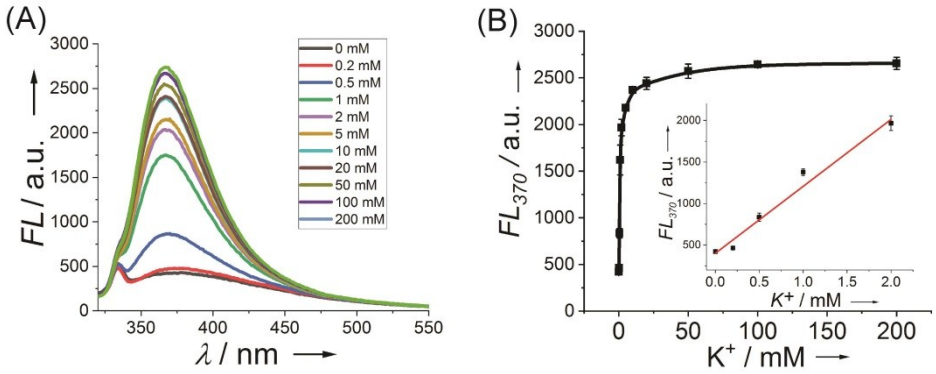

Figure S7. Application of this G-quadruplex probe to the analysis of K^+ in freshly collected lake water. (A) Fluorescence emission spectra of fluorogenic FG9A by adding increasing concentrations of K^+ (0 to 200 mM) into the working system. (B) Relationship between the fluorescence intensity of 2-AP at 370 nm and the K^+ concentration. The inset shows a linear relationship in the concentration range of K^+ from 0.2 mM to 2 mM. Error bar represents the standard deviation (n = 3).

Table S1. Comparison with other G-quadruplex based fluorescent method for K^+ detection.

Method	Detection limit	Linear range
PPIX binding K^+-stabilized parallel G-quadruplex[11]	0.5 mM	2–20 mM
G-quadruplex lighting up thioflavin T for "turn on" detection of K^+[12]	1 mM	0.1–20 mM
pyrene-labeled aptamer[13]	0.4 mM	0–20 mM
fluorescein-labeled G-quadruplex[14]	~mM	2–10 mM
this work	25 μM	0.1–2 mM

II. Materials

Oligonucleotide sequences

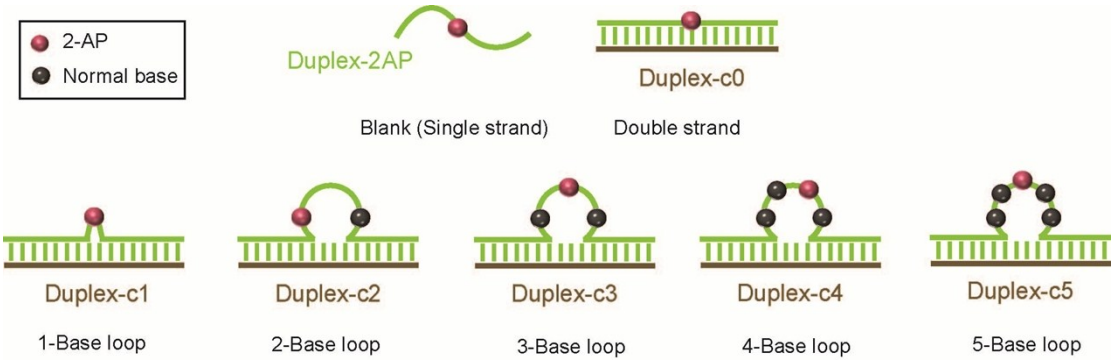

Figure S8. DNA sequences of 2-AP loop in duplex study.

Table S2. The DNA sequences of 2-AP loop in duplex study.

Name	Sequence (5'-3')
Cytosine-Duplex-2AP	CCTTTCCCCTTCTTTCCA_pCCTTTCTTCCCCTTTCC
Cytosine-Duplex-c0	GGAAAGGGGAAGAAAGGTGGAAAGAAGGGGAAAGG
Cytosine-Duplex-c1	GGAAAGGGGAAGAAAGGGGAAAGAAGGGGAAAGG
Cytosine-Duplex-c2	GGAAAGGGGAAGAAAGGGAAAGAAGGGGAAAGG
Cytosine-Duplex-c3	GGAAAGGGGAAGAAAGGAAAGAAGGGGAAAGG
Cytosine-Duplex-c4	GGAAAGGGGAAGAAAGAAAGAAGGGGAAAGG
Cytosine-Duplex-c5	GGAAAGGGGAAGAAAAAAGAAGGGGAAAGG
Thymine-Duplex-2AP	CCTTTCCCCTTCTCCTTA_pTTCCTCTTCCCCTTTCC
Thymine-Duplex-c0	GGAAAGGGGAAGAGGAATAAGGAGAAGGGGAAAGG
Thymine-Duplex-c1	GGAAAGGGGAAGAGGAAAAGGAGAAGGGGAAAGG
Thymine-Duplex-c2	GGAAAGGGGAAGAGGAAAGGAGAAGGGGAAAGG
Thymine-Duplex-c3	GGAAAGGGGAAGAGGAAGGAGAAGGGGAAAGG
Thymine-Duplex-c4	GGAAAGGGGAAGAGGAGGAGAAGGGGAAAGG
Thymine-Duplex-c5	GGAAAGGGGAAGAGGGGAGAAGGGGAAAGG
Guanine-Duplex-2AP	CCTTTCCCCTTCTTTGGA_pGGTTTCTTCCCCTTTCC
Guanine-Duplex-c0	GGAAAGGGGAAGAAACCTCCAAAGAAGGGGAAAGG
Guanine-Duplex-c1	GGAAAGGGGAAGAAACCCCAAAGAAGGGGAAAGG
Guanine-Duplex-c2	GGAAAGGGGAAGAAACCCAAAGAAGGGGAAAGG
Guanine-Duplex-c3	GGAAAGGGGAAGAAACCAAAGAAGGGGAAAGG
Guanine-Duplex-c4	GGAAAGGGGAAGAAACAAAGAAGGGGAAAGG
Guanine-Duplex-c5	GGAAAGGGGAAGAAAAAAGAAGGGGAAAGG

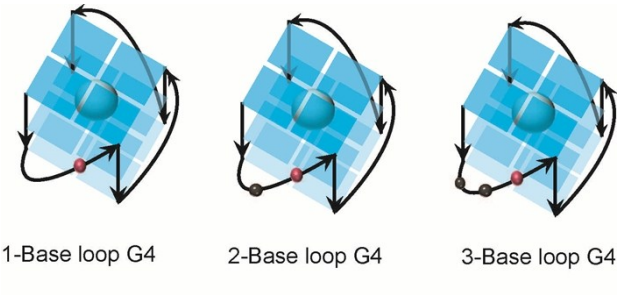

Figure S9. DNA sequences of 2-AP loop size study in G-quadruplex.

Table S3. DNA sequences of 2-AP loop in G-quadruplex study.

Name	Sequence (5'-3')
PW17	GGGTAGGGCGGGTTGGG
FG5A	GGGTA$_p$GGGCGGGTTGGG
FG9A	GGGTAGGGA$_p$GGGTTGGG
T30177	GTGGTGGGTGGGTGGGT
T30177-TT	TTGTGGTGGGTGGGTGGGT
FG6A	GGGTTA$_p$GGGTGGGTGGG
FG10A	GGGTGGGTTA$_p$GGGTGGG
FG14A	GGGTGGGTGGGTTA$_p$GGG
1-Base loop G4	GGGA$_p$GGGCGGGTTGGG
2-Base loop G4	GGGTA$_p$GGGCGGGTTGGG
3-Base loop G4	GGGTTA$_p$GGGTGGGTGGG
Human Telomere-1	TAGGGTTA$_p$GGGTTAGGGTTAGGG
Human Telomere-2	TAGGGTTAGGGTTA$_p$GGGTTAGGG
Human Telomere-3	TAGGGTTAGGGTTAGGGTTA$_p$GGG

The colored base indicates the 2-aminopurine substitution.

III. References

1. T. Li, E. Wang and S. Dong, *J. Am. Chem. Soc.*, 2009, **131**, 15082-15083.
2. Y. Xue, Z. Y. Kan, Q. Wang, Y. Yao, J. Liu, Y. H. Hao and Z. Tan, *J. Am. Chem. Soc.*, 2007, **129**, 11185-11191.
3. D. C. Ward, E. Reich and L. Stryer, *J Biol Chem*, 1969, **244**, 1228-1237.
4. B. Holz, *Nucleic Acids Res.*, 1998, **26**, 1076-1083.
5. E. L. Rachofsky, R. Osman and J. B. A. Ross, *Biochemistry*, 2001, **40**, 946-956.
6. L. Serrano-Andres, M. Merchan and A. C. Borin, *Proc. Natl. Acad. Sci. U. S. A.*, 2006, **103**, 8691-8696.
7. M. C. Miller, R. Buscaglia, J. B. Chaires, A. N. Lane and J. O. Trent, *J. Am. Chem. Soc.*, 2010, **132**, 17105-17107.
8. V. Dapic, V. Abdomerovic, R. Marrington, J. Peberdy, A. Rodger, J. O. Trent and P. J. Bates, *Nucleic Acids Res.*, 2003, **31**, 2097-2107.
9. V. Dapic, P. J. Bates, J. O. Trent, A. Rodger, S. D. Thomas and D. M. Miller, *Biochemistry*, 2002, **41**, 3676-3685.
10. N. Jing, R. F. Rando, Y. Pommier and M. E. Hogan, *Biochemistry*, 1997, **36**, 12498-12505.
11. T. Li, E. Wang and S. Dong, *Anal. Chem.*, 2010, **82**, 7576-7580.
12. L. Liu, Y. Shao, J. Peng, C. Huang, H. Liu and L. Zhang, *Anal. Chem.*, 2014, **86**, 1622-1631.
13. C. Shi, H. Gu and C. Ma, *Anal. Biochem.*, 2010, **400**, 99-102.
14. S. Nagatoishi, T. Nojima, E. Galezowska, A. Gluszynska, B. Juskowiak and S. Takenaka, *Anal. Chim. Acta*, 2007, **581**, 125-131.